

Article

The Influence of Lamina Density and Occurrence on the Permeability of Lamellar Shale after Hydration

Pengfei Zhao ^{1,2}, Xingxing Wang ³, Xiangyu Fan ^{1,2,3,*}, Xingzhi Wang ², Feitao Zeng ⁴, Mingming Zhang ³, Fan Meng ² and Wen Nie ^{1,5}

¹ State Key Laboratory of Oil and Gas Reservoir Geology and Exploitation, Southwest Petroleum University, Chengdu 610500, China; pfzhao@swpu.edu.cn (P.Z.); wen.nie@fjirsm.ac.cn (W.N.)

² School of Geoscience and Technology, Southwest Petroleum University, Chengdu 610500, China; 198431010017@swpu.edu.cn (X.W.); 202111000048@stu.swpu.edu.cn (F.M.)

³ Petroleum Engineering School, Southwest Petroleum University, Chengdu 610500, China; 202021000712@stu.swpu.edu.cn (X.W.); 201911000092@stu.swpu.edu.cn (M.Z.)

⁴ Department of Civil, Geological and Mining Engineering, École Polytechnique de Montréal, Montreal, QC H3T 1J4, Canada; feitao.zeng@polymtl.ca

⁵ School of Resources and Environmental Engineering, Jiangxi University of Science and Technology, Ganzhou 341000, China

* Correspondence: 199931010004@swpu.edu.cn; Tel.: +86-02883037050

Abstract: The characteristics of laminae in lamellar shale oil reservoirs have important influences on reservoir parameters, especially permeability. In order to explore the influence of lamina density and occurrence on the permeability of lamellar shale after hydration, we studied the lamellar shale in the Chang 7 member of the Yanchang Formation of Triassic in Ordos Basin. By comparing the permeability of bedding shale and lamellar shale with different densities of laminae, it was found that the permeability anisotropy of lamellar shale was stronger. In the direction parallel to the lamina, the permeability increased approximately linearly with an increase in lamina density. The effect of hydration on rock micropore structure and permeability was studied by soaking shale in different fluids. Most of the microfracture in the lamellar shale was parallel to the lamina direction, and hydration led to a widening of the microfracture, which led to the most obvious increase in permeability parallel to the lamina. Collectively, the research results proved that lamina density, occurrence, and hydration have a significant influence on the permeability anisotropy of lamellar shale.

Keywords: hydration; lamellar shale; Ordos Basin; permeability



Citation: Zhao, P.; Wang, X.; Fan, X.; Wang, X.; Zeng, F.; Zhang, M.; Meng, F.; Nie, W. The Influence of Lamina Density and Occurrence on the Permeability of Lamellar Shale after Hydration. *Crystals* **2021**, *11*, 1524. <https://doi.org/10.3390/cryst11121524>

Academic Editors: Carlos Rodriguez-Navarro and Per-Lennart Larsson

Received: 25 October 2021

Accepted: 26 November 2021

Published: 7 December 2021

Publisher's Note: MDPI stays neutral with regard to jurisdictional claims in published maps and institutional affiliations.



Copyright: © 2021 by the authors. Licensee MDPI, Basel, Switzerland. This article is an open access article distributed under the terms and conditions of the Creative Commons Attribution (CC BY) license (<https://creativecommons.org/licenses/by/4.0/>).

1. Introduction

Shale permeability is an important parameter for productivity evaluation and economic development of shale reservoirs [1,2]. While a shale reservoir is usually dense, with low matrix permeability and high clay content, its permeability is greatly affected by bedding occurrence and hydration of rock [3–5]. The type of lamellar shale that has developed in the continental shale oil reservoirs in China contains a lot of silty and tuffaceous laminae, which lead to the development of microfractures and stronger shale anisotropy and is more vulnerable to hydration [6,7]. Under the influence of lamina density (the number of laminae contained in unit thickness stratum) and occurrence (the angle between the lamina plane and horizontal plane), the permeability law of lamellar shale becomes more complicated.

Shale anisotropy is related to the development of weak plane structure, which is an important factor affecting the physical and mechanical properties of rock [8–10]. The clay content of continental shale is high, and the changes of rock structure and properties caused by clay hydration and expansion are also the key points related to the study of shale [11,12]. The mechanical behavior of shale is significantly affected by anisotropy and

hydration [13,14]. In the process of water absorption, shale specimens mainly expand and fail parallel to the bedding plane. Water absorption parallel to the bedding plane will enhance the influence of anisotropy on the geological mechanical behavior of shale [15]. Gui et al. studied the effect of hydration on the anisotropic damage of shale and found that the damage of parallel bedding was greater than that of vertical bedding [16,17], and the damage occurred in the early stage of hydration [18]. For lamellar shale, the structure of laminae determines the reservoir quality and oil potential of the shale, and the permeability difference of shale exists in different laminae and different positions of the same lamina [19,20]. In addition, shale permeability is significantly affected by pressure, and the apparent permeability of shale increases significantly with a decrease in pressure, i.e., at low pressure [21–23].

The pore structure of shale is the main factor affecting the storage capacity and production performance of shale gas reservoirs [24–26]. Shale contains a large number of nanoscale pores, and the abundance and maturity of organic matter are the main factors controlling the micropore structure of shale [27]. Zhang et al. quantitatively divided fluid occurrence and pore system in the shale of the Lower Silurian Longmaxi Formation in the southern Sichuan Basin and discussed the impact of disconnected pores on shale gas development [28]. Jiang et al. believed that the pore and fracture evolution process of shale under triaxial stress conditions could be divided into an initial stage, expansion stage, and permeability stage [29]. The characteristics of the micropore structure of shale are important factors that determine the permeability of the shale. Observations by scanning electron microscope have found that microfractures and a large number of intergranular pores occur parallel to the shale bedding plane, which all create the main channel for fluid flow [30]. The intergranular pores tend to be aligned, and the clay mineral particles parallel to the bedding are preferentially aligned [31]. After water saturation, the connectivity of the entire shale pore-fracture system is significantly increased, and the microfractures show a preferred direction or arrangement parallel to the shale bedding plane [32]. Hydration can promote the expansion of original fractures, and also induce new microfractures or branches [33], and the direction of bedding is the main factor controlling the direction of fracture propagation [34]. Hydration is conducive to fracturing shale gas reservoirs, to achieve the goal of increasing production [35].

At present, studies on the permeability characteristics of shale have mainly revolved around bedding shale, and there have been few studies on the permeability law of lamellar shale. In particular, the existing studies have not revealed the influence of the characteristics of lamina density and occurrence on rock permeability before and after hydration. Therefore, the lamellar shale in the third submember of the Chang 7 of the Triassic Yanchang Formation in Ordos Basin was used as the research object. The polarizing microscope and scanning electron microscopes were used to observe the micropore structure changes before and after hydration of the shale. Combined with experimental tests, the influence of the development characteristics of lamina and hydration time on rock porosity and permeability were analyzed, which provided support for the drilling and development of lamellar shale oil reservoirs.

2. Samples and Methods

2.1. Samples

Ordos Basin is one of the main oil and gas resource reservoir basins in China. Among them, the third submember of the Chang 7 member of the Triassic Yanchang Formation is a lamellar shale oil reservoir, mainly composed of shale, containing a small amount of siltstone and tuff. A large section of shale contains siltstone laminae, leading to the development of microfractures in the reservoir and strong rock anisotropy. The mineral composition of the reservoir is diverse, in which the contents of clay and quartz are prominent. The average content of clay is 31%, and some layers can reach 44% clay. The clay is mainly composed of illite and illite/smectite mixed layers (Figure 1).

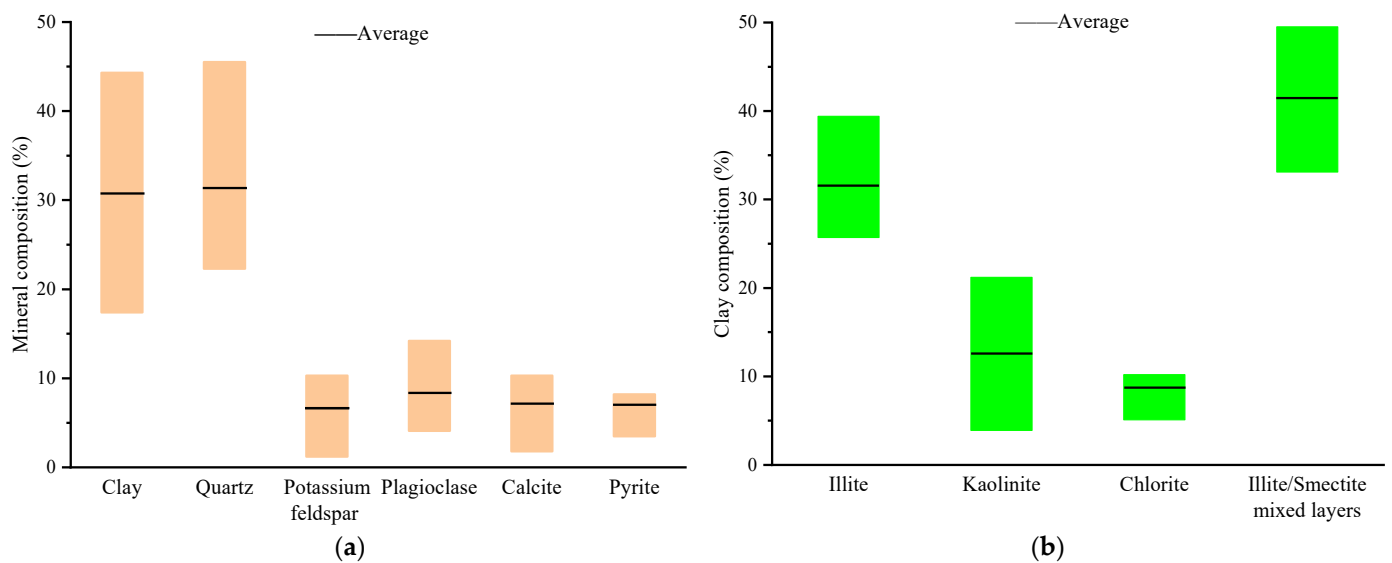


Figure 1. Mineral content of the third submember of the Chang 7 member: (a) Mineral content fluctuation diagram; (b) clay content fluctuation diagram.

There are lamellar shale and bedding shale (shale without laminae) in the whole reservoir. In the lamellar shale, the distances between laminae are also different, which is expressed by the lamina density in this research. In order to explore the effect of lamina density on permeability, bedding shale and lamellar shale with different densities of lamina were taken as experimental objects. In order to explore the permeability anisotropy, samples with different angles between the axial direction and the lamina plane were taken as the experimental objects (Figure 2).

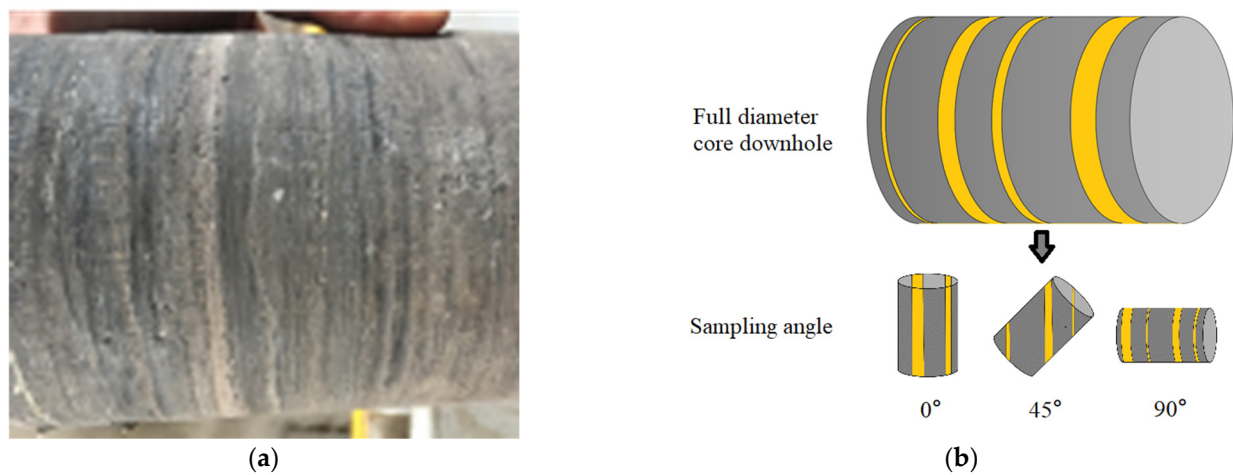


Figure 2. Full diameter core downhole and sample drilling processing method: (a) Full diameter core downhole; (b) sample drilling processing method.

2.2. Experimental Programs and Methods

In order to study shale micropore structure before and after hydration, three rock thin sections were treated, respectively, with no soaking, water soaking at 90 °C for 48 h, and water-based drilling fluid soaking at 90 °C for 48 h, and then the rock thin section observation was performed to compare and analyze the samples before and after hydration. Similarly, three micro square core samples were treated, respectively, with no soaking, water soaking at 90 °C for 24 h, and water-based drilling fluid soaking at 90 °C for 24 h,

and the micropore structure before and after hydration was observed by scanning electron microscope.

In order to study the effect of hydration on rock porosity, 4 samples were taken; 2 samples were soaked in 80 °C water, and 2 samples were soaked in 80 °C water-based drilling fluid. Their initial porosity and porosity after 12, 24, 36, and 48 h of soaking were tested, sequentially.

In order to study the influence of lamina density on the permeability of hydrated shale, samples with different densities of lamina and occurrences were used to test their initial permeability and the permeability after soaking in water and water-based drilling fluid for 12, 24, 36, and 48 h. The water-based drilling fluid in this experiment was an inhibitory water-based drilling fluid with amino inhibitor and nanosilica.

2.2.1. Observation Experiment of Rock Thin Section

When colored liquid glue is injected into rock pore space under vacuum pressure, the pore characteristics of a sample can be observed with a microscope after the liquid glue is cured [36]. In this study, the rock was prepared in 0.5 mm thin sections by grinding, and then blue glue was injected into the rock thin sections by a ZT-2 high pressure casting instrument. Finally, the fracture and pore structure of the rock thin sections were observed under a BX51-P-DP12 polarizing microscope.

2.2.2. Core Scanning Electron Microscope Analysis Experiment

Scanning electron microscopy (SEM) can emit electrons and receive reaction signals from the observed samples, and these signals can characterize certain physical or chemical properties of the rock surface, which is an important method for studying rock pore structure [37]. In this study, the rock was processed into the micro square core with a side length of 1 cm through a sander and an LEICA EM TIC 3X three-ion beam cutter. The LEICA EM ACE 200 type coating instrument was used to spray gold on the observation surface to ensure a clear image during observation and the sample was observed by FEI Quanta 650 FEG field emission scanning electron microscope.

2.2.3. Porosity Experiment

At a constant temperature, the pressure and volume of the gas are inversely proportional, and the total porosity of the rock can be measured by the dual-chamber method [33]. An HEP-P porosity tester was used to test rock porosity. Before the experiment, the cylindrical core of the measured size was put into the sample chamber, and helium was added into the reference chamber at a predetermined pressure (100~200 psi). After the pressure was balanced, the pressure P_1 was read out. Then, the gas expanded into the sample chamber, and the pressure measured after equilibrium was P_2 . The total porosity of the rock could be calculated by Equation (1) [38] as follows:

$$\Phi = \left(\frac{V_C P_1}{P_2} + V_{00} - V_C - V_Y \right) / V_0 \quad (1)$$

where Φ is the porosity of the test sample, V_{00} is the volume of the test sample, V_C is the volume of the reference chamber, V_Y is the volume of the sample chamber, P_1 is the first balance pressure, and P_2 is the second balance pressure.

2.2.4. Permeability Experiment

According to Darcy's law, the seepage velocity of porous media is directly proportional to the cross-sectional area, pressure difference, and permeability, and inversely proportional to the viscosity and length of the porous media [39]. In the experiment, shale permeability was tested using a Gasperm steady-state gas permeability meter, with a test temperature of 20 °C and a pressure of 230 psi. The permeability ratio of the parallel lamina and the vertical lamina was used to express the permeability anisotropy of the lamellar shale [40].

3. Results

3.1. Observation Results of Rock Thin Sections

Figure 3 shows the results of rock thin sections before and after soaking. From the results, it could be concluded that the microfracture in samples developed parallel to the lamina or at a small angle with the lamina whether soaking or not. As compared with that before soaking (Figure 3a), the microfracture in the rock after soaking in water expanded and widened, and new fractures were generated nearby (Figure 3b). The samples soaked in drilling fluid were covered and blocked by argillaceous and solid particles in the drilling fluid, and there were no obvious fractures on the surface (Figure 3c).

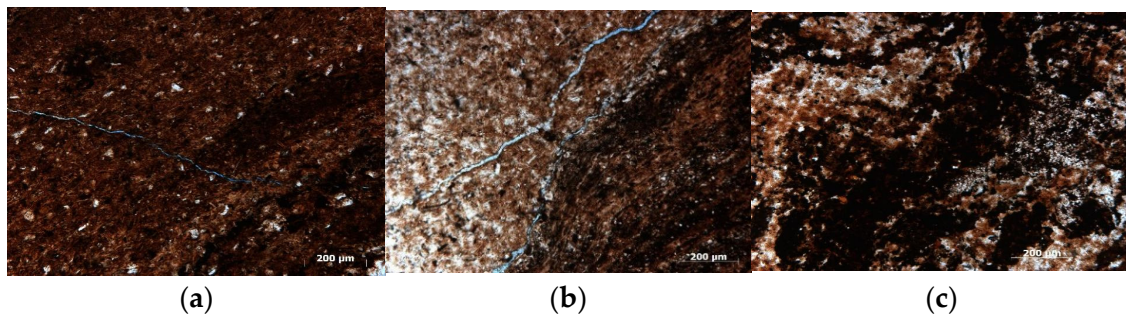


Figure 3. Results of casting thin section identification: (a) 0° sample without soaking treatment; (b) 45° sample soaked in water at room temperature for 48 h; (c) 45° sample soaked in drilling fluid at room temperature for 48 h.

3.2. SEM Experimental Results

Figure 4 shows the SEM experimental results of the sample with a lamina angle of 45° after soaking in 90°C water and 90°C drilling fluid for 24 h. The results showed that the direction of fractures and mineral arrangement on the sample surface were consistent with the lamina occurrence (Figure 4a), and these fractures could reach more than 700 nm. After soaking in water, some pores on the rock surface were connected to form a large area of holes (Figure 4c). The fractures in some samples was warped on the observation surface and delamination occurred. (Figure 4d). After soaking in drilling fluid, the drilling fluid formed mud cake on the sample surface to prevent debris particles from falling off (Figure 4e), and the solid particles penetrated into the fractures and pores to form plugging (Figure 4f).

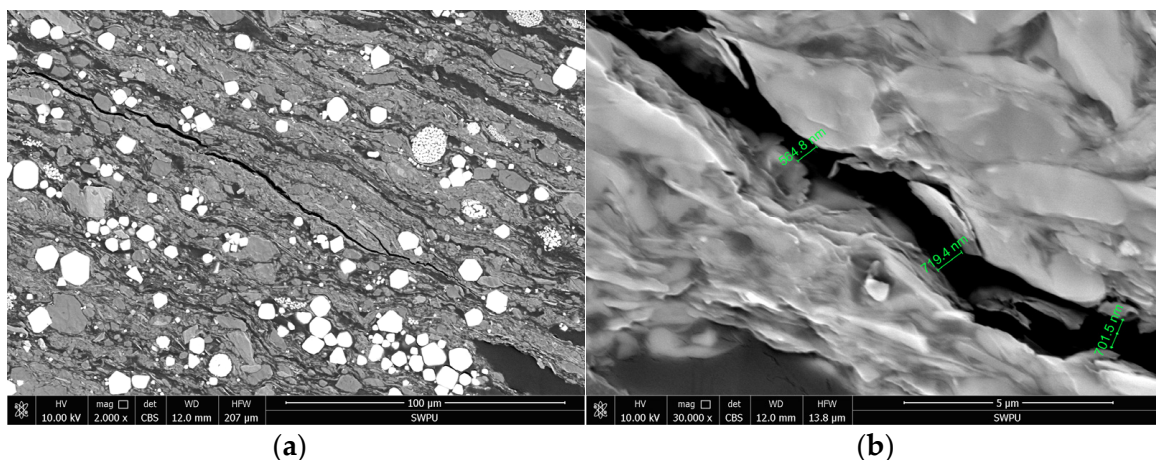


Figure 4. Cont.

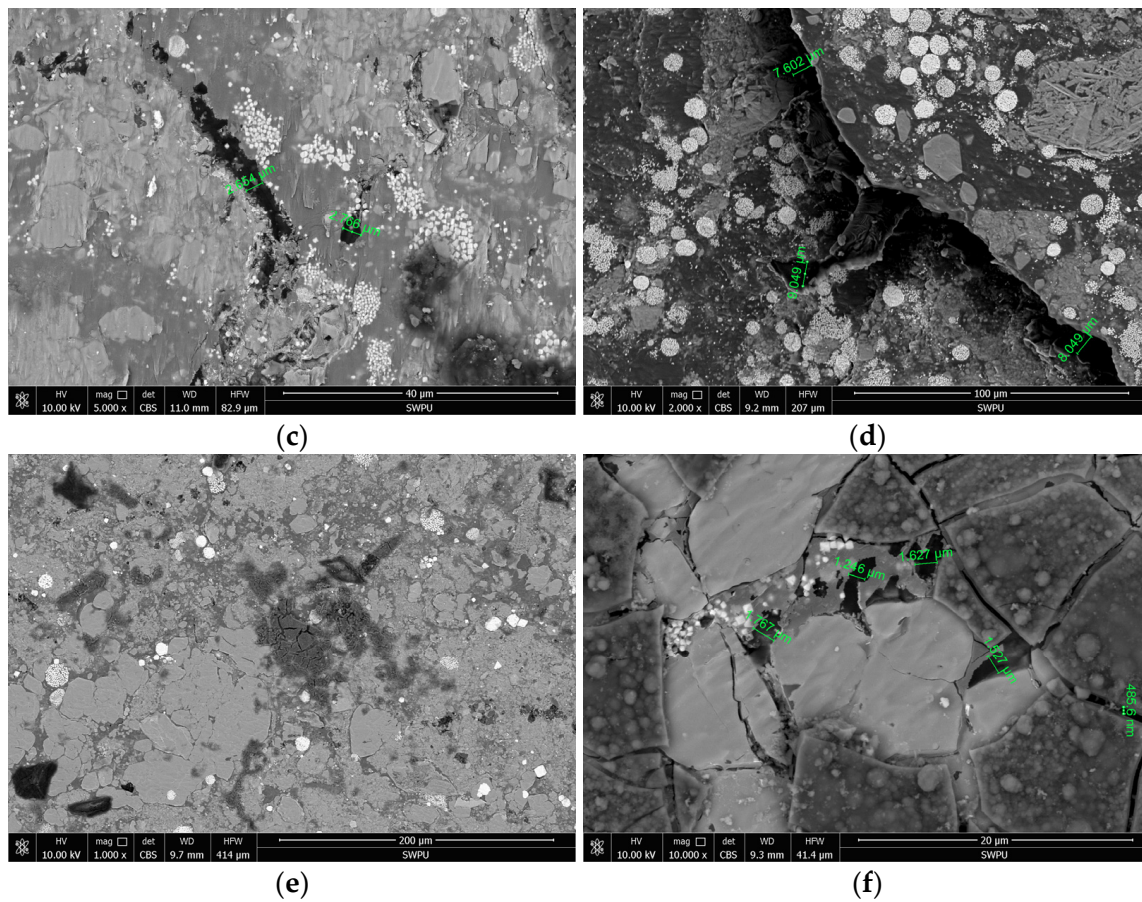


Figure 4. SEM experimental results of lamellar shales under 45° lamina occurrence: (a) Flat bedding fractures without soaking treatment; (b) nanoscale bedding fractures without soaking treatment; (c) surface debris spalling after soaking in water; (d) delamination occurs after soaking in water; (e) filling of debris surface by drilling fluid; (f) sealing of micro-scale fractures with drilling fluid materials.

3.3. Experimental Results of Porosity

After testing the initial total porosity of the samples, the samples were soaked in water at 80 °C or drilling fluid at 80 °C for different periods of time. After drying, the porosity results of samples could be observed, as shown in Figure 5. From the results of the porosity experiments, it could be seen that the porosity of shale reservoirs increased with an increase in soaking time, indicating that shale hydration would increase porosity. The porosity of the lamellar shale soaked in water changed significantly with an increase in time, while the change range of the lamellar shale soaked in drilling fluid was relatively stable with an increase in time. In bedding shale, there were similar laws, which indicated that the type of soaking liquid had an important influence on the porosity change of shale after hydrated. In the first 12 h of water soaking, the lamellar shale sample increased from an initial porosity of 1.65% to 2.51%, and the bedding shale sample increased from an initial porosity of 0.66% to 1.24. During the period of 36–48 h of soaking in water, the porosity of the lamellar shale sample only increased from 2.91% to 2.95%, and the porosity of the bedding shale sample only increased from 1.44% to 1.45%. The change of porosity mainly occurred in the early stage of soaking, and the porosity remained basically unchanged at the later stage of soaking, which meant that the porosity of samples increased nonlinearly with an increase in soaking time. As compared with the porosity changes in the samples, it was found that drilling fluid reduced the rate of porosity growth, indicating that the drilling fluid weakened the hydration of the core.

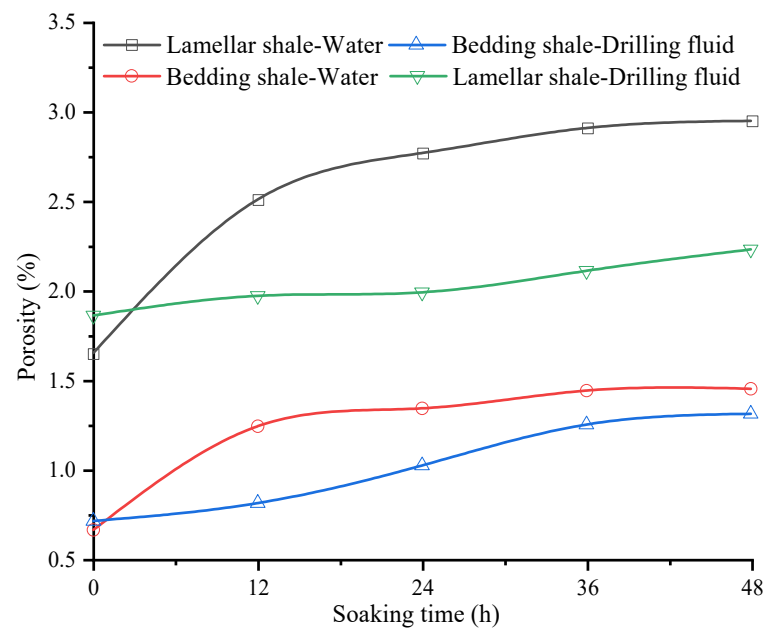


Figure 5. Relationship between shale porosity and soaking time under 0° sampling.

3.4. Permeability Test Results

3.4.1. Experimental Results of Hydration Permeability under the Different Lamina Densities

The lamina density was related to the sampling angle, and the lamina density of bedding shale was zero. When the 50 × 25 mm cylinder samples were drilled at the same place in the full diameter core, the lamina density in 45° and 90° samples was similar, which was twice that in 0° samples. The experimental results of permeability with different densities of lamin (Figure 6) showed that shale permeability increased with an increase in lamina density, whether in water or drilling fluid. The permeability increased linearly with an increase in lamina density, especially in the direction parallel to the laminae. When sampling at 0° (Figure 6a), the permeability increased significantly with an increase in the lamina density, but the influence of fluid type was not great, indicating that the lamina density had a greater impact on the hydration permeability of the shale when sampling at 0° than the soaking fluid type. When sampling at 45° (Figure 6b), the permeability change caused by lamina density from 0 to 2 was not obvious, but the change became obvious when the lamina density increased to 4. When sampling at 90°, the increase in permeability of samples soaked in water was significantly higher than that of samples soaked in drilling fluid, while the increase in permeability caused by an increase in lamina density was much lower than that when the sample angles were 0° and 45°. The result showed that, when the sampling angle was 90°, the influence of hydration on the permeability of lamellar shale was greater than that of lamina density, and the type of soaking fluid played a leading role in the permeability change of lamellar shale.

3.4.2. Experimental Results of Hydration Permeability under Different Occurrences

The experimental results of hydration permeability under different sampling angles (Figure 7) showed that the permeability after hydration decreased with an increase in the sampling angle. The permeability was the largest at 0° and the permeability at 90° was the smallest, that is, under the same lamina density, the permeability in the parallel lamina direction was the largest, and the permeability in the vertical lamina direction was the smallest. The permeability growth rate of samples in drilling fluid was smaller than that of samples in water at the same lamina density and sampling angle, especially when the sampling angle was 0°, which proved that drilling fluid had the best effect on inhibiting the permeability growth in the parallel lamina direction. The permeability of lamellar shale had a larger variation range than that of bedding shale, which proved that the existence

of laminae increased the influence of hydration on rock permeability. When the sampling angle increased, the permeability dropped sharply, while the influence of fluid type was relatively small. It showed that the influence of lamina direction on the shale permeability after hydration was greater than that of the soaking fluid type.

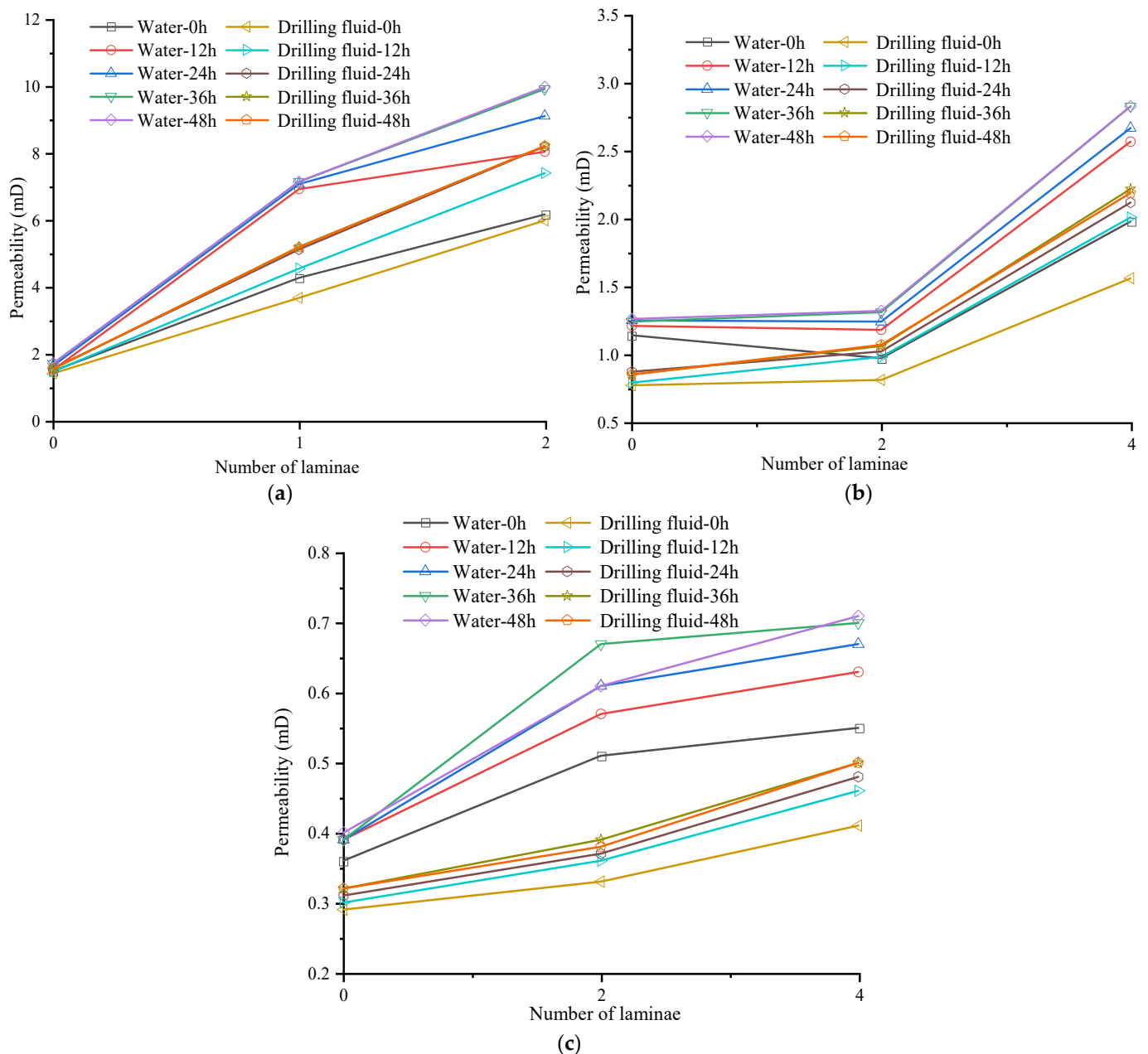


Figure 6. Permeability under the different lamina densities: (a) The relationship between density and permeability of rock samples under 0° sampling; (b) the relationship between density and permeability of rock samples under 45° sampling; (c) the relationship between density and permeability of rock samples under 90° sampling.

3.4.3. Experimental Results of Hydration Permeability under Different Soaking Times

The experimental results of hydration permeability under different soaking times (Figure 8) showed that shale permeability increased with an increase in soaking time, which proved that hydration would increase the permeability of shale oil reservoir rocks. When the lamina density in the lamellar shale sample was one, the permeability of lamellar shale changed nonlinearly with soaking time. The permeability of lamellar shale increased from

4.27 mD to 6.93 mD after soaking in water for 12 h, and the permeability of lamellar shale only increased from 6.93 mD to 7.15 mD after soaking in water for 12–48 h, which indicated that the influence of hydration on the permeability of lamellar shale mainly occurred in the early stage. Under the same soaking time and lamina direction, the permeability of samples soaked in drilling fluid was less than that in water, indicating that the drilling fluid could inhibit the hydration of shale.

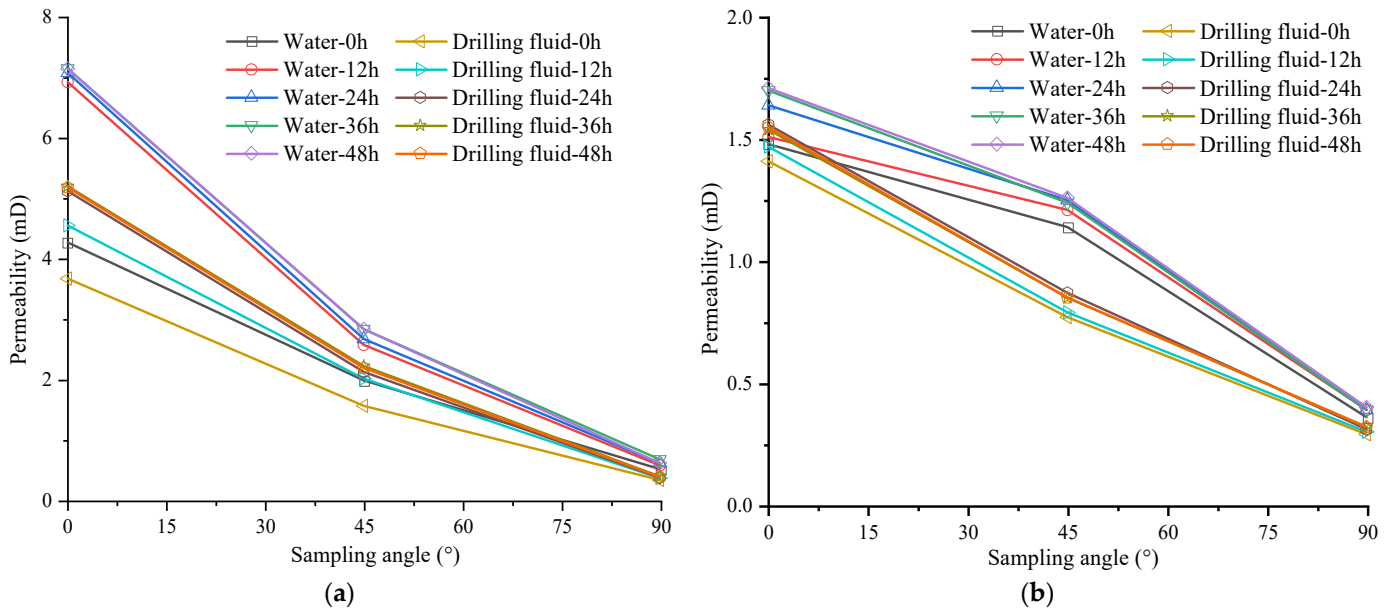


Figure 7. Permeability under the different sampling angles: (a) The relationship between permeability and sampling angle of lamellar shale, the lamina density with sampling angle of 0° is 1, the lamina density with sampling angle of 45° and 90° is 2; (b) the relationship between permeability and sampling angle of bedding shale.

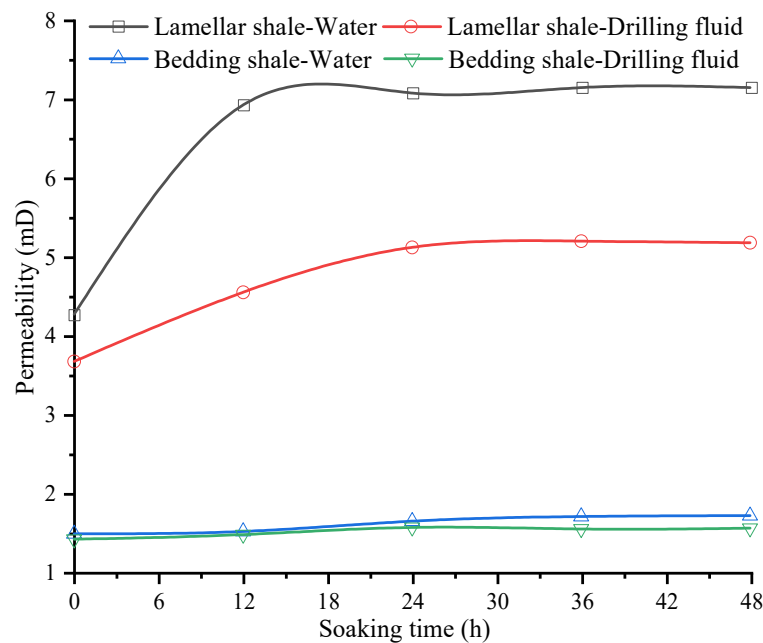


Figure 8. The relationship between permeability and soaking time under 0° sampling, the lamina density in the lamellar shale sample is 1.

4. Discussion

4.1. The Relationship between Hydration Micropore Structure and Permeability

There were a lot of clastic minerals in continental lamellar shale oil reservoir, and the cementation ability between minerals was weak. After soaking, clastic minerals were easy to fall off the rock surface, which increased the micropores in the rock and the appearance of new pores further aggravated rock hydration. The content of clay minerals in the reservoir was high; after the clay was soaked in water, the cementing ability decreased, and the minerals attached to the clay easily fell off, further aggravating the internal hydration of the rock. When the fracture made contact with the fluid, the hydration further increased the length and opening of the fracture, resulting in a high permeability fracture net.

The drilling fluid formed a protective mud cake on the rock surface, which could reduce the contact area between the fluid and the rock, enhanced the cementing ability of minerals and clays, and inhibited the hydration of the rock surface. Solid particles and soil powder accumulated in fractures, reduced the permeability of fractures, reduced the contact between the fracture surface and the drilling fluid, and inhibited the internal hydration of the rock. The hydration inhibitor in the drilling fluid reduced the hydration expansion and dispersion ability of the clay, and reduced the osmotic hydration of shale [41]. The use of inhibitory drilling fluids in drilling operations can effectively ensure the stability of the wellbore.

4.2. Considering the Influence Mechanism of Shale Lamina Occurrence and Density on Permeability

The degree of laminar microfracture development was the main factor affecting expansion, providing channels for fluid to enter the rock, which greatly increased the contact between fluid and rock. When the laminae and microfractures met water, the weak cementation surface between different lithologies was easy to separate and form fractures. The greater the lamina density, the larger the contact area between fluid and rock, resulting in an increase in porosity and permeability.

The micropore structure of lamellar shale showed that microfractures that provided permeability for the rock were mainly developed parallel to the lamina and distributed near the lamina interface, resulting in an increase in rock permeability with an increase in lamina density, which was consistent with the experimental results of permeability. After being hydrated, it was also easy to produce new fractures near the lamina interface, which further increased the permeability of the rock parallel to the laminar direction. The permeability of rock in the lamina direction was significantly higher than that in the direction normal to the lamina, which was the reason for the anisotropic increase in permeability of lamellar shale after hydration.

4.3. Permeability Anisotropy

Figure 9 shows the permeability anisotropy of shale under different lamina densities and different fluid soaking conditions. It can be seen that the relationship between permeability anisotropy of shale and soaking time is not a simple positive correlation or negative correlation, which is related to the changes in micropore structure of rocks in different fluids and different soaking time periods. The lamellar shale had a larger change in permeability anisotropy than bedding shale. Among them, the changes in permeability anisotropy for lamellar shale and bedding shale soaked in water for 48 h were 3.35 and 0.17, respectively, which proved that the shale containing laminae would increase the permeability anisotropy. Under the same lithology and lamina development, the influence of drilling fluid on the permeability anisotropy of the sample was less than that in water, which proved that hydration increased the permeability anisotropy of shale oil reservoir rocks. This effect could be reduced by adding drilling fluids with inhibitors and plugging agents.

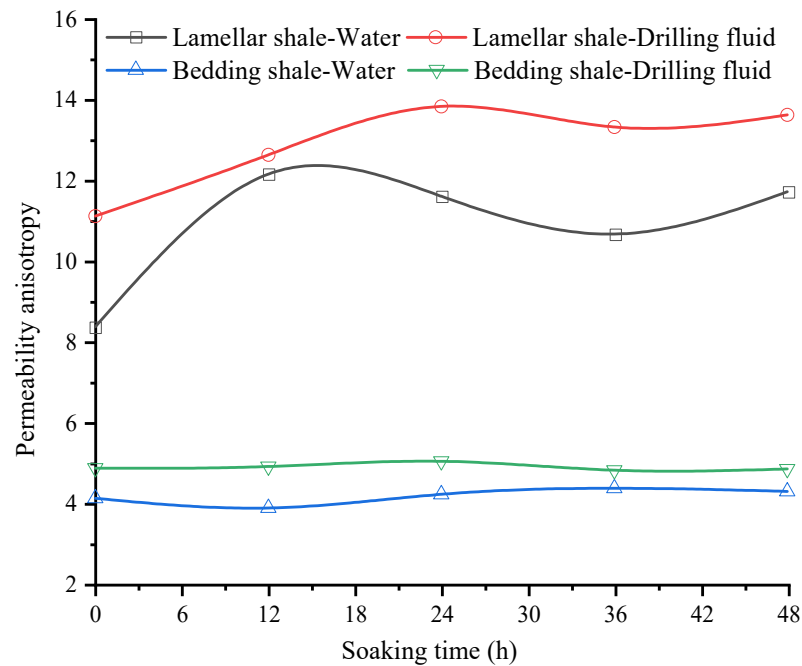


Figure 9. The influence of different lamina developments and soaking fluids on permeability anisotropy, the lamina density with sampling angle of 0° is 1, the lamina density with sampling angle of 90° is 2.

5. Conclusions

In this study, we took the shale oil reservoir core of the third submember of the Chang 7 member in the Ordos Basin as the research object. We analyzed the micropore structure of the rock before and after hydration through rock thin section identification and scanning electron microscope, and tested the development characteristics of the lamina and the influence of hydration on rock permeability. The results are as follows:

1. The lamina density and occurrence had a significant impact on the permeability of shale. The permeability of the rock increased approximately linearly with the lamina density, especially in the direction parallel to the laminae. The occurrence of laminae was the main reason for the permeability anisotropy of rock, and the permeability parallel to the lamina direction could reach ten times the permeability in the direction normal to the lamina.
2. After the lamellar shale was soaked in water, the dissolution pores between the rock particles became more obvious. There were stratifications inside the rock and the fractures along the laminae became longer and wider. The change of this structure led to a significant increase in permeability, especially in the direction parallel to the lamina.
3. With an increase in hydration time, the permeability of rock showed a trend that first increased and then tended to be stable. As compared with bedding shale, the permeability of lamellar shale was more susceptible to hydration, and the shale permeability in the direction parallel to the laminae was more susceptible to hydration.

Author Contributions: Conceptualization, P.Z. and X.W. (Xingxing Wang); methodology, X.F.; software, M.Z.; validation, F.Z. and M.Z.; formal analysis, X.W. (Xingxing Wang); investigation, X.W. (Xingzhi Wang); resources, W.N.; data curation, P.Z.; writing—original draft preparation, X.W. (Xingxing Wang); writing—review and editing, P.Z.; visualization, F.M.; supervision, X.F.; project administration, X.F. and W.N.; funding acquisition, X.F. and W.N. All authors have read and agreed to the published version of the manuscript.

Funding: This research was funded by the financial supports from the Open Fund (PLN1502) of the State Key Laboratory of the Oil and Gas Reservoir Geology and Exploitation, Southwest Petroleum University and the National Natural Science Foundation of china (grant nos. 51774246 and 42172313).

Institutional Review Board Statement: Not applicable.

Informed Consent Statement: Not applicable.

Data Availability Statement: Not applicable.

Acknowledgments: The financial supports from the Open Fund (PLN1502) of the State Key Laboratory of the Oil and Gas Reservoir Geology and Exploitation, Southwest Petroleum University and the National Natural Science Foundation of china (grant nos. 51774246 and 42172313) are appreciated. The authors would like to express their gratitude to the editors and anonymous reviewers for their constructive comments on the draft paper.

Conflicts of Interest: The authors declare no conflict of interest.

References

1. Yang, S.; Yin, P.; Xu, S. Permeability Evolution Characteristics of Intact and Fractured Shale Specimens. *Rock Mech. Rock Eng.* **2021**, 1–20. [[CrossRef](#)]
2. Zhou, J.; Tian, S.; Zhou, L.; Xian, X.; Yang, K.; Jiang, Y.; Zhang, C.; Guo, Y. Experimental investigation on the influence of sub- and super-critical CO₂ saturation time on the permeability of fractured shale. *Energy* **2020**, *191*, 116574. [[CrossRef](#)]
3. Lu, J.; Jiang, C.; Jin, Z.; Wang, W.; Zhuang, W.; Yu, H. Three-dimensional physical model experiment of mining-induced deformation and failure characteristics of roof and floor in deep underground coal seams. *Process Saf. Environ. Prot.* **2021**, *150*, 400–415. [[CrossRef](#)]
4. Jiang, C.; Yang, Y.; Wei, W.; Duan, M.; Yu, T. A new stress-damage-flow coupling model and the damage characterization of raw coal under loading and unloading conditions. *Int. J. Rock Mech. Min. Sci.* **2021**, *138*, 104601. [[CrossRef](#)]
5. Jiang, C.; Liu, C.; Shang, X. Double event joint location method considering P-wave arrival time system errors. *Soil Dyn. Earthq. Eng.* **2021**, *149*, 106890. [[CrossRef](#)]
6. Liu, B.; Sun, J.; Zhang, Y.; He, J.; Fu, X.; Yang, L.; Xing, J.; Zhao, X. Spatial types and enrichment models of shale oil in the 1st member of Qingshankou Formation of Cretaceous in Changling Sag, Songliao Basin. *Pet. Explor. Dev.* **2021**, *48*, 521–535. [[CrossRef](#)]
7. Zhao, X.; Pu, X.; Zhou, L.; Jin, F.; Han, G.; Shi, Z.; Han, W.; Ding, Y.; Zhang, W.; Wang, G.; et al. The theory, exploration technology and prospects of shale oil enrichment in deep basin lacustrine area: Taking the Paleogene in Huanghua Depression of Bohai Bay Basin as an example. *Acta Pet. Sin.* **2021**, *42*, 143–162.
8. Ma, T.; Zhang, Q.; Chen, P.; Yang, C.; Zhao, J. Fracture pressure model for inclined wells in layered formations with anisotropic rock strengths. *J. Pet. Sci. Eng.* **2017**, *149*, 393–408. [[CrossRef](#)]
9. Ma, T.; Wu, B.; Fu, J.; Zhang, Q.; Chen, P. Fracture pressure prediction for layered formations with anisotropic rock strengths. *J. Nat. Gas Sci. Eng.* **2017**, *38*, 485–503. [[CrossRef](#)]
10. Ma, T.; Liu, Y.; Chen, P.; Wu, B.; Fu, J.; Guo, Z. Fracture-initiation pressure prediction for transversely isotropic formations. *J. Pet. Sci. Eng.* **2019**, *176*, 821–835. [[CrossRef](#)]
11. Zhang, Y.; Li, T.; Xie, L.; Yang, Z.; Li, R. Shale lamina thickness study based on micro-scale image processing of thin sections. *J. Nat. Gas Sci. Eng.* **2017**, *46*, 817–829. [[CrossRef](#)]
12. Guillermina, M.; Viviana, R.; Zbyšek, P.; Milena, P.; Edgardo, F.I. Assessment of packing, flowability, hydration kinetics, and strength of blended cements with illitic calcined shale. *Constr. Build. Mater.* **2020**, *254*, 119042. [[CrossRef](#)]
13. Zhang, Q.; Yao, B.; Fan, X.; Li, Y.; Li, M.; Zeng, H.; Zhao, P. A modified Hoek-Brown failure criterion for unsaturated intact shale considering the effects of anisotropy and hydration. *Eng. Fract. Mech.* **2021**, *241*, 107369. [[CrossRef](#)]
14. Zhang, Q.; Fan, X.; Chen, P.; Ma, T.; Zeng, F. Geomechanical behaviors of shale after water absorption considering the combined effect of anisotropy and hydration. *Eng. Geol.* **2020**, *269*, 105547. [[CrossRef](#)]
15. Ma, T.; Peng, N.; Zhu, Z.; Zhang, Q.; Yang, C.; Jian, Z. Brazilian Tensile Strength of Anisotropic Rocks: Review and New Insights. *Energies* **2018**, *11*, 304. [[CrossRef](#)]
16. Gui, J.; Ma, T.; Chen, P.; Yuan, H.; Guo, Z. Anisotropic Damage to Hard Brittle Shale with Stress and Hydration Coupling. *Energies* **2018**, *11*, 926. [[CrossRef](#)]
17. You, L.; Xie, B.; Yang, J.; Kang, Y.; Han, H.; Wang, L.; Yang, B. Mechanism of fracture damage induced by fracturing fluid flowback in shale gas reservoirs. *Nat. Gas Ind. B* **2018**, *38*, 61–69. [[CrossRef](#)]
18. Ma, T.; Yang, C.; Chen, P.; Wang, X.; Guo, Y. On the damage constitutive model for hydrated shale using CT scanning technology. *J. Nat. Gas Sci. Eng.* **2016**, *28*, 204–214. [[CrossRef](#)]
19. Wang, S.; Wang, G.; Huang, L.; Song, L.; Zhang, Y.; Li, D.; Huang, Y. Logging evaluation of lamina structure and reservoir quality in shale oil reservoir of Fengcheng Formation in Mahu Sag, China. *Mar. Pet. Geol.* **2021**, *133*, 105299. [[CrossRef](#)]

20. Liang, C.; Cao, Y.; Liu, K.; Jiang, Z.; Wu, J.; Hao, F. Diagenetic variation at the lamina scale in lacustrine organic-rich shales: Implications for hydrocarbon migration and accumulation. *Geochim. Cosmochim. Acta* **2018**, *229*, 112–128. [[CrossRef](#)]
21. Chen, Y.; Jiang, C.; Leung, J.Y.; Wojtanowicz, A.K.; Zhang, D.; Zhong, C. Second-order correction of Klinkenberg equation and its experimental verification on gas shale with respect to anisotropic stress. *J. Nat. Gas Sci. Eng.* **2021**, *89*, 103880. [[CrossRef](#)]
22. Yin, C. Test and analysis on the permeability of induced fractures in shale reservoirs. *Nat. Gas Ind. B* **2018**, *5*, 513–522. [[CrossRef](#)]
23. Hu, Z.; Duan, X.; He, Y.; Wu, J.; Chang, J.; Liu, L.; Wu, K.; Ma, Z. Influence of reservoir primary water on shale gas occurrence and flow capacity. *Nat. Gas Ind. B* **2019**, *6*, 71–78. [[CrossRef](#)]
24. Guo, X.; Li, Y.; Liu, R.; Wang, Q. Characteristics and controlling factors of micropore structures of the Longmaxi Shale in the Jiaoshiha area, Sichuan Basin. *Nat. Gas Ind. B* **2014**, *1*, 165–171. [[CrossRef](#)]
25. Yang, Y.; Jiang, C.; Guo, X.; Peng, S.; Zhao, J.; Yan, F. Experimental investigation on the permeability and damage characteristics of raw coal under tiered cyclic unloading and loading confining pressure. *Powder Technol.* **2021**, *389*, 416–429. [[CrossRef](#)]
26. Jiang, C.; Wang, Y.; Duan, M.; Guo, X.; Chen, Y.; Yang, Y. Experimental study on the evolution of pore–fracture structures and mechanism of permeability enhancement in coal under cyclic thermal shock. *Fuel* **2021**, *304*, 121455. [[CrossRef](#)]
27. Chen, Y.; Jiang, C.; Leung, J.Y.; Wojtanowicz, A.K.; Zhang, D. Gas slippage in anisotropically-stressed shale: An experimental study. *J. Pet. Sci. Eng.* **2020**, *195*, 107620. [[CrossRef](#)]
28. Zhang, H.; Jiang, Y.; Zhou, K.; Fu, Y.; Zhong, Z.; Zhang, X.; Qi, L.; Wang, Z.; Jiang, Z. Connectivity of pores in shale reservoirs and its implications for the development of shale gas: A case study of the Lower Silurian Longmaxi Formation in the southern Sichuan Basin. *Nat. Gas Ind. B* **2020**, *7*, 348–357. [[CrossRef](#)]
29. Jiang, C.; Liu, X.; Wang, W.; Wei, W.; Duan, M. Three-dimensional visualization of the evolution of pores and fractures in reservoir rocks under triaxial stress. *Powder Technol.* **2021**, *378*, 585–592. [[CrossRef](#)]
30. Chen, Y.; Jiang, C.; Yin, G.; Wojtanowicz, A.K.; Zhang, D.M. Permeability and Effective Stress in Dipping Gas Shale Formation With Bedding—Experimental Study. *J. Energy Resour. Technol.* **2020**, *142*, 1–36. [[CrossRef](#)]
31. Chen, Y.; Jiang, C.; Yin, G.; Zhang, D.; Xing, H.; Wei, A. Permeability evolution under true triaxial stress conditions of Longmaxi shale in the Sichuan Basin, Southwest China. *Powder Technol.* **2019**, *354*, 601–614. [[CrossRef](#)]
32. Chen, Y.; Jiang, C.; Leung, J.Y.; Wojtanowicz, A.K.; Zhang, D. Multiscale characterization of shale pore–fracture system: Geological controls on gas transport and pore size classification in shale reservoirs. *J. Pet. Sci. Eng.* **2021**, *202*, 108442. [[CrossRef](#)]
33. Yang, H.; Shi, X.; Yin, C.; Liang, X.; Zhao, J.; Li, J.; Zhu, J.; Geng, Z.; Wu, Z.; Li, R. Brazilian tensile failure characteristics of marine shale under the hydration effect of different fluids. *Nat. Gas Ind. B* **2020**, *7*, 639–647. [[CrossRef](#)]
34. Sun, K.; Zhang, S.; Xin, L. Impacts of bedding directions of shale gas reservoirs on hydraulically induced crack propagation. *Nat. Gas Ind. B* **2016**, *3*, 139–145. [[CrossRef](#)]
35. Song, F.; Xiao, H.; Ji, K.; Huang, X. Effect of fluid–solid coupling on shale mechanics and seepage laws. *Nat. Gas Ind. B* **2018**, *5*, 41–47. [[CrossRef](#)]
36. Wang, R.; Ding, W.; Zhang, Y.; Wang, Z.; Wang, X.; He, J.; Zeng, W.; Dai, P. Analysis of developmental characteristics and dominant factors of fractures in Lower Cambrian marine shale reservoirs: A case study of Niutitang formation in Cen’gong block, southern China. *J. Pet. Sci. Eng.* **2016**, *138*, 31–49. [[CrossRef](#)]
37. Tang, X.; Zhu, Y.; Liu, Y. Investigation of shale nano-pore characteristics by scanning electron microscope and low-pressure nitrogen adsorption. *J. Nanosci. Nanotechnol.* **2017**, *17*, 6252–6261. [[CrossRef](#)]
38. Voorn, M.; Exner, U.; Barnhoorn, A.; Baud, P.; Reuschlé, T. Porosity, permeability and 3D fracture network characterisation of dolomite reservoir rock samples. *J. Pet. Sci. Eng.* **2015**, *127*, 270–285. [[CrossRef](#)]
39. Sheng, G.; Javadpour, F.; Su, Y. Dynamic porosity and apparent permeability in porous organic matter of shale gas reservoirs. *Fuel* **2019**, *251*, 341–351. [[CrossRef](#)]
40. Zhao, P.; Fan, X.; Zhang, Q.; Yao, B.; Zhang, M.; He, L.; Qiang, Y.; Liu, J. Characteristics of Hydration Damage and Its Influence on Permeability of Lamellar Shale Oil Reservoirs in Ordos Basin. *Geofluids* **2021**, *2021*, 1–15. [[CrossRef](#)]
41. Wang, B.; Sun, J.; Shen, F.; Li, W.; Zhang, W. Mechanism of wellbore instability in continental shale gas horizontal sections and its water-based drilling fluid countermeasures. *Nat. Gas Ind. B* **2020**, *7*, 680–688. [[CrossRef](#)]